RESEARCH PAPERS

Acta Cryst. (1995). B**51**, 908–913

Structure Determination of $CuTh_2(PO_4)_3$

BY M. LOUËR, R. BROCHU AND D. LOUËR

Laboratoire de Cristallochimie, CSIM (URA CNRS 1495), Université de Rennes I, Avenue du Général Leclerc, 35042 Rennes CEDEX, France

AND S. ARSALANE AND M. ZIYAD

Laboratoire de Catalyse, Faculté des Sciences, Avenue Ibn Batouta, Rabat, Morocco

(*Received* 17 *October* 1994; *accepted* 2 *February* 1995)

Abstract

The crystal structure of $CuTh_2(PO_4)_3$, copper dithorium triphosphate, has been solved *ab initio* from conventional monochromatic X-ray powder diffraction and refined with neutron powder diffraction data. The symmetry is monoclinic, space group $C2/c$. The heavy-atom positions were found from a Patterson map calculated from integrated intensities extracted by whole-pattern fitting. Successive Fourier syntheses were used to locate the remaining atoms. The Th atoms and PO_4 groups exhibit an arrangement related to that found in the $M^1Th_2(PO_4)_3$ phases, with large sites in which the monovalent cations are located. In the title compound, these sites are elongated along **a** and shortened along **b** so that the Cu^+ ions, located on inversion centres, are linearly bonded to two phosphate groups with two short Cu—O distances of 1.828 Å.

Introduction

A number of copper (I) monophosphates have been reported, *e.g.* $CuM_2^{IV}(PO_4)_3$ (M = Ti, Zr, Sn, Th), $Cu_{1-x}Nb_xTi_{2-x}(PO_4)_3$, $Cu_{1+x}M_{2-x}Cr_x(PO_4)_3$ and $H_{0.5}Cu_{0.5}M_2(PO_4)_3$ [M = Ti, Zr (El Jazouli, Serghini, Brochu, Dance & Le Flem, 1985; Mbandza, Bordes & Courtine, 1987; Yao & Fray, 1983; Serghini, 1984; Serghini, Brochu, Gravereau & Olazcuaga, 1995; Schmid & Mooney, 1964; Le Polles *et al.*, 1987; McCarron, Calabrese & Subramanian, 1987]. Among them, $CuTh_2(PO_4)_3$ and $CuZr_2(PO_4)_3$ exhibit interesting fluorescence properties (Schmid & Mooney, 1964; Le Polles, Parent, Olazcuaga, Le Flem & Hagenmuller, 1988). $CuZr_2(PO_4)_3$ is also an active catalyst of the 2-butanol conversion with an aperiodic oscillatory behaviour (Serghini, Kacimi, Ziyad & Brochu, 1988). The Nasicon-type structure of $CuZr_2(PO_4)_3$ has been recently refined from X-ray and neutron powder diffraction data (Bussereau *et al.*, 1992). The $CuTh_2(PO_4)_3$ phase reported first by Schmidt & Mooney (1964) does not belong to this family. Its X-ray powder diffraction pattern was indexed with a monoclinic unit cell (Cc or $C2/c$) by Laügt (1973), suggesting similarities with the structure of the $M^1Th_2(PO_4)_3$ Matkovic phases [M^1 = K, Tl, Na, Li (Matkovic, Prodic & Sljukic, 1968)]. Preliminary studies on the catalytic activity of $CuTh_2(PO_4)_2$ show promising properties, due to a better dispersion of the metallic copper particles on the surface compared with that observed for $CuZr_2(PO_4)_3$ (Arsalane, Kacimi, Ziyad, Coudurier & Vedrine, 1995). To our knowledge no complete structural study has been published, probably because single crystals of this phase were reported to be obtained only in micaceous intergrown flakes or grains (Keester & Jacobs, 1974). The present study deals with the structure of $CuTh_2(PO_4)_3$, solved *ab initio* from conventional X-ray powder diffraction data and refined by the Rietveld method from neutron powder diffraction data.

Experimental

$CuTh_2(PO_4)_3$ was obtained by a sol–gel-type method. The starting compounds $Th(NO_3)_4.5H_2O$ and $Cu(NO_3)_2.3H_2O$ were separately dissolved in a reduced volume of distilled water and mixed in stoichiometric proportions. The rapid addition of a solution of $(NH_4)_2HPO_4$ produced a transparent bluish gel. This gel was maintained at 343 K for 24 h and then progressively heated to 673 K; the powder was finally calcined at 1273 K in air for 48 h with no extra precaution, leading to a whitish compound. Nevertheless, an analysis of the EPR spectra of the final product revealed a very small amount of copper(II), probably localized on the surface (Arsalane, Kacimi, Ziyad, Coudurier & Vedrine, 1995).

X-ray powder diffraction data were collected with a Siemens D500 high-resolution powder diffractometer using monochromatic Cu $K\alpha_1$ radiation (λ = 1.540598 Å) obtained with an incident-beam germanium

ISSN 0108-7681

monochromator. Characteristics of the diffractometer and its instrument resolution curve, showing a shallow minimum of 0.065° (2θ) at *ca* 40° (2θ), have been described elsewhere (Louër & Langford, 1988). The diffraction pattern was scanned over the angular range 8–129°(2θ) with a step of 0.02° (2θ). The counting times were 23.5 s step^{-1} to 80° and 47 s step^{-1} from 80.02° to the end of the scan. Then, the full pattern was scaled to the lower counting time. For pattern indexing, the precise determination of peak positions was carried out by means of the Socabim fitting program *PROFILE*, available in the PC software package *DIFFRAC-AT* supplied by Siemens.

Neutron powder diffraction data were collected, at room temperature, with the high-resolution multidetector powder diffractometer D1A (λ = 1.8876 Å) of the Laboratoire Léon Brillouin (Laboratoire commun CEA-CNRS). The pattern was scanned over the range 10–156° (2θ) with a step length of 0.05° (2θ).

Table 1. *Details of the Rietveld refinements from X-ray and neutron powder diffraction data for* $CuTh_2(PO_4)_3$; *the unit cell is derived from the X-ray data*

a (Å)	22.0291 (8)
b (Å)	6.7430 (4)
c (Å)	7.0191 (4)
β (°)	108.58 (1)
V (Å^3)	988.1 (4)
Z	4
Space group	$C2/c$
No. of atoms	10

	X-ray	Neutrons
Wavelength (Å)	1.5406	1.8876
2θ range (°)	8–129	10–156
Step scan increment, 2θ (°)	0.02	0.05
No. of reflections	834	572
No. of structural parameters	29*	36
R_F	0.04	0.03
R_B	0.07	0.05
R_P	0.13	0.07
R_{WP}	0.18	0.09

* An overall B (for P and O atoms) and two isotropic (for Th and Cu) temperature factors were refined with the X-ray diffraction data set.

Data analysis

Powder pattern indexing

Indexing of the X-ray powder diffraction pattern was performed by means of the program *DICVOL91* (Boultif & Louër, 1991) from the first 20 lines, with an absolute error of 0.03° (2θ) on measured peak positions. Two solutions with high figures of merit were obtained:

Orthorhombic symmetry: $a = 20.874\,(1)$, $b = 6.7437\,(5)$, $c = 7.0192\,(6)$ Å, $V = 988.1$ Å^3, Bravais lattice I, $Z = 4$, $M_{20} = 114$, $F_{20} = 168$ (0.0021, 57).

Monoclinic symmetry: $a = 22.022\,(2)$, $b = 6.7433\,(8)$, $c = 7.0196\,(10)$ Å, $\beta = 108.58\,(1)°$, $V = 988.1$ Å^3, Bravais lattice C, $Z = 4$, $M_{20} = 89$, $F_{20} = 126\,(0.0018, 87)$.

Inspection of the indices of observed reflections suggested the space groups *Ima*2 or *Imam* for the orthorhombic solution and *Cc* or *C*2/*c* for the monoclinic cell were suggested. In fact, these two solutions are related since the (pseudo-) orthorhombic cell can be deduced from the monoclinic one by the transformation matrix: 1,0,1/0,1,0/0,0,1. The monoclinic cell agrees with the unit cell reported previously by Laügt (1973). The structure solution described in the present study shows that the correct solution is the monoclinic cell. The cell parameters refined from the complete data set are given in Table 1. On the other hand, there is no evidence for an isostructural relationship with the unit cells of the $AB_2(PO_4)_3$ compounds [A = K, Na, Ag; B = U, Th, Ce (Keester & Jacobs, 1974)], since the a axis and β angle are greater in the monoclinic unit cell of $CuTh_2(PO_4)_3$.

Structure solution and refinement

The extraction of the integrated intensities from the X-ray powder diffraction pattern has been carried out by means of an automatic iterative fitting procedure available in the program *FULLPROF* (Rodriguez-Carvajal, 1990), considering in a first stage the indexing solution with the highest symmetry, orthorhombic with the space group *Imam*. 486 'F_{obs}' values were obtained and introduced in the structure determination package *MolEN* (Fair, 1990), running on a MicroVAX computer. The Th atom was located by interpretation of the Patterson function. The Cu atom and two PO_4 groups were found by several Fourier maps alternating with least-squares Rietveld refinements; however, attempts to locate the last PO_4 group failed, in spite of trying several orthorhombic space groups. Consequently, in a second stage, the atomic coordinates of Th and Cu were transformed to be in accordance with the monoclinic *C*2/*c* space group, and then from a Fourier map the remaining atoms were found. In all, a total of 10 atoms were found in the asymmetric unit, and this structure model was then refined by the Rietveld method. 45 parameters were used in the final Rietveld refinement: 29 structural parameters (including a scale factor, two isotropic thermal parameters for Th and Cu atoms, one overall isotropic temperature factor for the remaining atoms), the zero-point and four cell parameters, three coefficients to describe the angular dependence of line breadths, one asymmetry parameter, and two parameters to describe the angular variation of the mixing factor of the pseudo-Voigt function fitted to the observed diffraction lines. In addition, five coefficients were used to describe the functional dependence of the background (see Table 1). Fig. 1 shows the best fit between calculated and observed diffraction patterns, corresponding to satisfactory structure model and profile indicators $R_F = 0.04$ and $R_{wp} = 0.18$. The final positional parameters and temperature factors obtained from the X-ray diffraction data set are listed in Table 2. The precision with which light-atom positions have been determined from these

Table 2. *Fractional atomic coordinates and thermal isotropic parameters* ($Å^2$) *for* $CuTh_2(PO_4)_3$ *from X-ray (RX) and neutron (N) powder diffraction*

Note: in the refinement from the X-ray diffraction data, an overall isotropic factor, $B = 0.8(1)$ $Å^2$, was used for the P and O atoms.

		x	y	z	B_{iso}
Th	RX	0.36081 (6)	0.3574 (2)	0.8612 (5)	0.1 (1)
	N	0.3604 (1)	0.3578 (4)	0.8552 (5)	1.18 (6)
Cu	RX	0	1/2	1/2	2.6 (3)
	N	0	1/2	1/2	3.6 (1)
P1	RX	0.1804 (4)	0.323 (1)	0.673 (3)	
	N	0.1815 (2)	0.3222 (9)	0.683 (1)	1.4 (1)
P2	RX	1/2	0.361 (3)	1/4	
	N	1/2	0.359 (2)	1/4	2.9 (2)
O1	RX	0.138 (1)	0.513 (3)	0.606 (4)	
	N	0.1446 (3)	0.5139 (7)	0.6701 (9)	1.6 (1)
O2	RX	0.157 (1)	0.180 (5)	0.484 (4)	
	N	0.1540 (3)	0.182 (1)	0.4983 (9)	1.2 (1)
O3	RX	0.2491 (9)	0.358 (3)	0.718 (4)	
	N	0.2517 (2)	0.3605 (8)	0.7239 (9)	1.6 (1)
O4	RX	0.175 (1)	0.223 (5)	0.840 (5)	
	N	0.1722 (3)	0.193 (1)	0.8573 (9)	1.1 (1)
O5	RX	0.470 (1)	0.226 (3)	0.076 (3)	
	N	0.4669 (3)	0.230 (1)	0.0632 (9)	2.6 (1)
O6	RX	0.450 (1)	0.491 (4)	0.280 (4)	
	N	0.4444 (4)	0.486 (1)	0.265 (1)	3.2 (2)

X-ray data is low, as expected in the presence of much more strongly scattering Th atoms, and as shown by the range of the chemically equivalent P—O distances calculated from them, 1.39–1.59 Å. A similar problem is encountered in $U(UO_2)(PO_4)_2$ (Bénard *et al.*, 1994). Neutron diffraction data were therefore used for the further refinement of the atomic coordinates. The scattering lengths of Th and O atoms are in the ratio 1.78/1. A Gaussian function was selected to fit the individual line profiles. The angular dependence of the peak full width at half-maximum was described by the usual quadratic form in $\tan\theta$. Unit cell and instrumental parameters were allowed to vary from time to time during the refinement process. The final Rietveld refinement from the neutron data set involved the following parameters: 36 structural parameters (including 10 isotropic temperature factors), 14 instrumental parameters (including five coefficients to describe the functional dependence of the background). The details of the Rietveld refinement are given in Table 1.* Fig. 2 shows the final fit between calculated and observed patterns. It corresponds to satisfactory crystal structure model indicators R_B and R_F and profile factors R_P and R_{wp} (see Table 1). Final atomic parameters from X-ray and neutron diffraction data are given in Table 2. The standard deviations as obtained from the computer program may be multiplied by the correction factors 2.25 (X-ray data) and 1.82 (neutron data) to give 'probable errors' with regard to serial correlations as defined by Bérar & Lelann (1991). Then, most of the coordinates agree within 3 e.s.d.'s. As expected, the precision of the positions of O atoms derived from the X-ray diffraction data is lower than that from neutron diffraction data. The precision may be further decreased by the presence of an impurity phase (~1–2%) detected in the sample used in the X-ray diffraction study, as revealed by two spurious lines with low intensity at 10.25 and 22.27° (2θ; see Fig. 1). Selected interatomic distances and angles obtained with the neutron diffraction data set are given in Table 3, where it can be seen that the dimensions of the phosphate appear much more reasonable, with P—O distances ranging from 1.503 to 1.569 Å.

* Primary diffraction data have been deposited with the IUCr (Reference: HA0136). Copies may be obtained through The Managing Editor, International Union of Crystallography, 5 Abbey Square, Chester CH1 2HU, England.

Results and discussion

In the $M^1Th_2(PO_4)_3$ Matkovic phases, the packing of the Th atoms and PO_4 groups accommodates large sites in which the monovalent cations are located (Matkovic *et al.*, 1970). This framework is also found in the structure of $CuTh_2(PO_4)_3$. However, significant differences exist

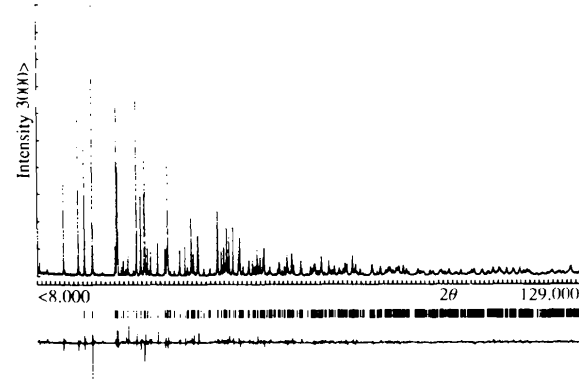

Fig. 1. Final Rietveld plot of $CuTh_2(PO_4)_3$ from monochromatic X-ray powder diffraction data. The upper trace shows the observed data as dots, while the calculated pattern is shown by a solid line. The lower trace is a plot of the difference: observed minus calculated. The vertical markers show positions calculated for Bragg reflections.

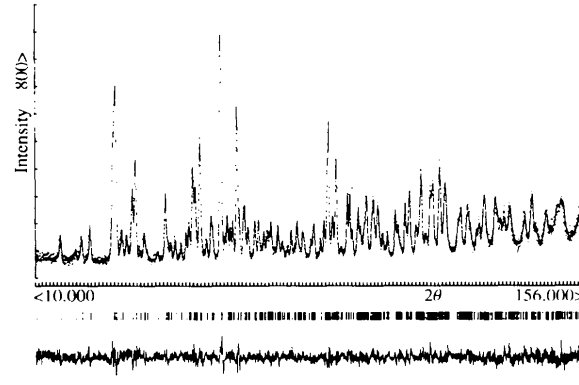

Fig. 2. Final Rietveld plot of $CuTh_2(PO_4)_3$ from neutron powder diffraction data. The upper trace shows the observed data as dots, while the calculated pattern is shown by a solid line. The lower trace is a plot of the difference: observed minus calculated. The vertical markers show positions calculated for Bragg reflections.

Table 3. *Selected distances* (Å) *and angles* (°) *for* $CuTh_2(PO_4)_3$ *(from the neutron data set)*

Th	—	O3	2.275 (6)
	—	$O1^{i}$	2.326 (5)
	—	$O4^{ii}$	2.372 (7)
	—	$O6^{iii}$	2.383 (9)
	—	$O2^{iv}$	2.414 (7)
	—	$O2^{v}$	2.481 (8)
	—	$O5^{vi}$	2.489 (7)
	—	$O4^{v}$	2.675 (7)
	—	$O6^{vi}$	3.010 (8)
$O1^{i}$	—	O3	3.186 (8)
	—	$O4^{ii}$	3.155 (9)
O3	—	$O4^{ii}$	2.905 (9)
$O4^{v}$	—	$O2^{v}$	2.422 (8)
	—	$O6^{iii}$	2.72 (1)
$O2^{v}$	—	$O6^{iii}$	3.321 (1)
$O4^{ii}$	$O1^{i}$	O3	54.5 (2)
$O1^{i}$	O3	$O4^{ii}$	62.2 (3)
O3	$O4^{ii}$	$O1^{i}$	63.3 (2)
$O2^{v}$	$O6^{iii}$	$O4^{v}$	46.0 (2)
$O6^{iii}$	$O4^{v}$	$O2^{v}$	80.4 (4)
$O4^{v}$	$O2^{v}$	$O6^{iii}$	53.7 (3)
Cu	—	$O5^{vii}$, $O5^{viii}$ (×2)	1.828 (7)
	—	O1, $O1^{ix}$ (×2)	3.025 (7)
P1	—	O1	1.514 (8)
	—	O2	1.561 (9)
	—	O3	1.503 (7)
	—	O4	1.569 (9)
P2	—	O5, $O5^{x}$ (×2)	1.55 (1)
	—	O6, $O6^{x}$ (×2)	1.52 (1)
O1	P1	O2	114.0 (9)
O1	P1	O3	111.4 (8)
O1	P1	O4	108.7 (8)
O2	P1	O3	111.4 (9)
O2	P1	O4	101.4 (8)
O3	P1	O4	109.2 (8)
O5	P2	$O5^{x}$	111 (1)
O5	P2	O6	102 (1)
$O5^{x}$	P2	$O6^{x}$	102 (1)
O5	P2	$O6^{x}$	115 (1)
$O5^{x}$	P2	O6	115 (1)
O6	P2	$O6^{x}$	112 (1)

Symmetry codes: (i) $\frac{1}{2}-x, y-\frac{1}{2}, \frac{3}{2}-z$; (ii) $\frac{1}{2}-x, \frac{1}{2}-y, 2-z$; (iii) $x, 1-y, \frac{1}{2}+z$; (iv) $\frac{1}{2}-x, \frac{1}{2}-y, 1-z$; (v) $\frac{1}{2}-x, \frac{1}{2}+y, \frac{3}{2}-z$; (vi) $x, y, 1+z$; (vii) $\frac{1}{2}-x, \frac{1}{2}+y, \frac{1}{2}-z$; (viii) $x-\frac{1}{2}, \frac{1}{2}-y, \frac{1}{2}+z$; (ix) $-x, 1-y, 1-z$; (x) $1-x, y, \frac{1}{2}-z$.

between the two structures. Fig. 3 displays a comparison of the structures of $NaTh_2(PO_4)_3$ and $CuTh_2(PO_4)_3$. $NaTh_2(PO_4)_3$ was described in the *C*2/*c* space group although a piezoelectric effect was reported. There is a disorder of the Na^+ ions located off the twofold axes at $z = \pm 0.348$ instead of ± 0.25, while Cu^+ is located on an inversion centre ($z = 0, 0.5$) in such a way that it adopts a linear coordination. It should also be noted that in $KTh_2(PO_4)_3$ K^+ is located on a twofold axis (Matkovic, Prodic, Sljukic & Peterson, 1968). In the two structures shown in Fig. 3 there are two independent phosphate groups. Cu^+ seems to 'attract' the PO_4 groups located on the twofold axes and to 'repulse' the other PO_4 groups. This fact is responsible for the differences observed in the positions of the phosphate groups and Th atoms with regard to their location in the Matkovic phases.

The Th atom is surrounded by eight O atoms in a distance range 2.275 (6)–2.675 (7) Å, involving six monodentate and one bidentate phosphate groups. This environment could be described as a highly distorted bicapped trigonal prism (Fig. 4). The distortion of this polyhedron can be appreciated by the mean displacement of O atoms from the plane of the lateral faces [0.28 Å for $O6^{iii}$, $O2^{v}$, $O1^{i}$, $O4^{ii}$ (capped by $O5^{vi}$); 0.09 Å for

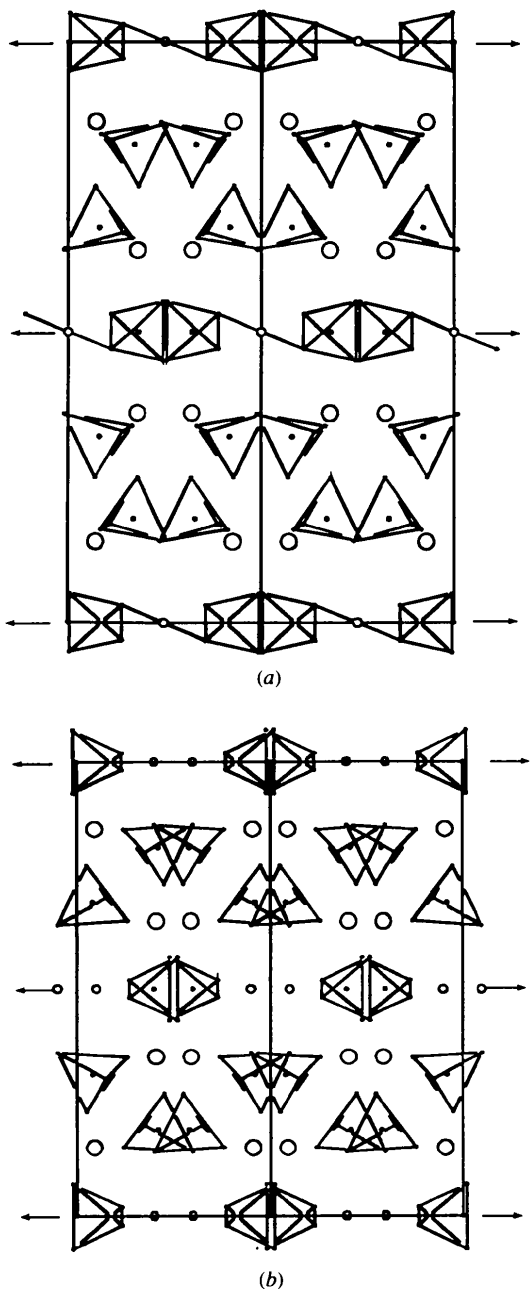

Fig. 3. Projection along [001] of two cells of (*a*) $CuTh_2(PO_4)_3$ and (*b*) $NaTh_2(PO_4)_3$. Large circles: Th; small circles: Cu or Na (the shorter *b* axis is horizontal).

$O6^{iii}$, $O4^{v}$, O3, $O1^{i}$ (capped by $O2^{iv}$) and 0.27 Å for $O4^{v}$, $O2^{v}$, $O4^{ii}$, O3] and by the distances and angles observed in the trigonal faces [$O1^{i}$, O3, $O4^{ii}$ and $O6^{iii}$, $O2^{v}$, $O4^{v}$ (see Table 3)]. The deviation angle of these trigonal faces from parallelism is 27°. The atoms $O2^{v}$ and $O4^{v}$ belong to the same PO_4 group; therefore, the shortest O—O distance (2.422 Å) has a major effect in the severe distortion of the polyhedron. The next closest O atom is $O6^{vi}$, located at 3.010 Å from Th (dashed line in Fig. 4). A similar situation has already been encountered in the structure of $Na_2Th(PO_4)_2$ (Galesic, Matkovic, Topic, Coffou & Sljukic, 1984), in which the two additional furthest O atoms lead to a coordination number changing from 8 to 10. The ThO_8 polyhedra are linked together by the PO_4 groups in the [100] and [010] directions. They have a common edge along [001], which would be a face if the $O6^{vi}$ atom were included in the coordination sphere of Th. Moreover, since $O6^{vi}$ and $O5^{vi}$ belong to the same phosphate group, the subsequent short O—O distance is responsible for the eccentricity of $O6^{vi}$ with respect to the third non-capped face ($O2^{v}$, $O4^{v}$, O3, $O4^{ii}$). Consequently, if the coordination number of Th is 9 in the Matkovic phases, it is more reasonable to consider a coordination number of 8 + 1 instead of 9 in the copper phase.

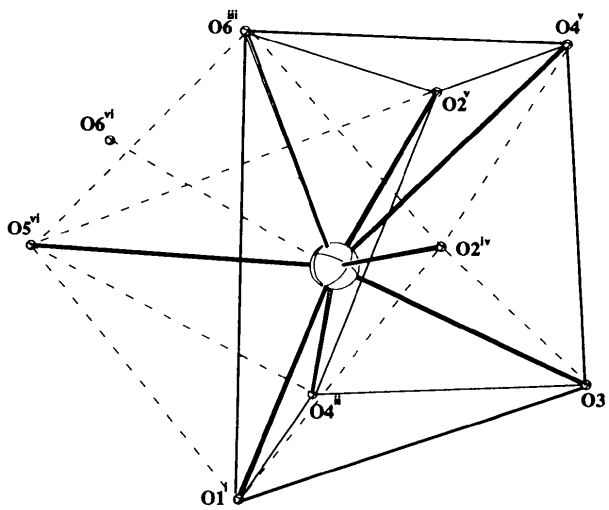

Fig. 4. The highly distorted trigonal prism around Th.

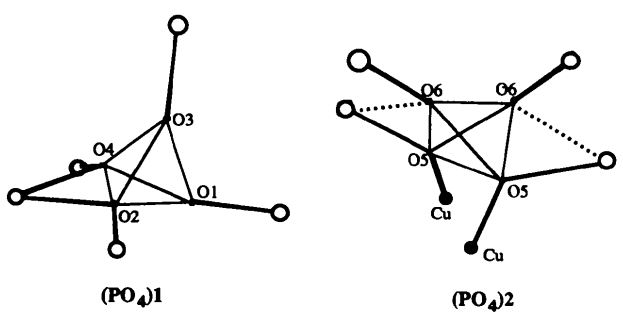

Fig. 5. Environment of the two independent phosphate groups.

The environment of the two independent phosphate groups $(PO_4)1$ and $(PO_4)2$ is represented in Fig. 5. $(PO_4)1$ is surrounded by five Th atoms and acts as a bidentate ligand for one of them. $(PO_4)2$ is surrounded by two Cu and four Th atoms; it is not a bidentate ligand if the two longest distances Th—O6 (dashed line) are not included in the coordination sphere of thorium.

The Cu atoms lie on inversion centres. These positions involve a linear coordination with a short Cu—O5 distance of 1.828 (7) Å. The next closest O atoms are O1 at 3.025 Å. Such a linear coordination is usual for Cu^{I}, *e.g.* in Cu_2O Cu has two collinear bonds (1.849 Å) and in oxides with the *delafossite* structure mean Cu—O distances are 1.798 Å in $CuScO_2$ and 1.861 Å in $CuAlO_2$ (Swanson & Fuyat, 1953; Ishiguro, Kitazawa, Mituzani & Kato, 1981). In the case of $Cu^{I}NbO_3$, the coordination around Cu is almost linear with an average Cu—O distance of 1.85 Å (Marinder & Wahlström, 1984).

$CuTh_2(PO_4)_3$ has been reported as non-piezoelectric (Laügt, 1973), which is consistent with the *C2/c* space group. Some authors have observed a disordered occupation of the sites in monovalent copper compounds, *e.g.* in $CuZr(PO_4)_3$ some sites may be vacant and others are filled by two close Cu^{+} forming a pair (Fargin *et al.*, 1994). Refinement in the space group *Cc* was attempted, but gave no evidence to suggest the Cu atoms are displaced from the site of symmetry $\bar{1}$ in *C2/c*.

To conclude, the Cu cation is definitely located on an inversion centre; this fact may be regarded as the essential difference between the structure of $CuTh_2(PO_4)_3$ and the Matkovic phases. Cu^{+} is then strongly bonded to two phosphate groups located on the twofold axis. The trend of Cu^{+} to be linearly bonded may explain the increasing of the *a* axis and the highly distorted Th–O polyhedron. At last, from the application of modern powder crystallography techniques, the crystal structure of copper thorium phosphate has been solved. It is worth noting that the structure solution was found from X-ray diffraction data collected with a high-resolution system using conventional monochromatic X-rays. The use of neutron diffraction data has contributed to improve the overall quality of the refinement of the atomic coordinates.

We are indebted to Dr J. Rodriguez-Carvajal from Laboratoire Léon Brillouin (Saclay, France) who kindly provided the neutron powder diffraction data, and to Professor D. Grandjean for helpful discussions.

References

ARSALANE, S., KACIMI, M., ZIYAD, M., COUDURIER, G. & VEDRINE, J. C. (1995). To be published.

BÉNARD, P., LOUËR, D., DACHEUX, N., BRANDEL, V. & GENET, M. (1994). *Chem. Mater.* **6**, 1049–1058.

BÉRAR, J. F. & LELANN, P. (1991). *J. Appl. Cryst.* **24**, 1–5.
BOULTIF, A. & LOUËR, D. (1991). *J. Appl. Cryst.* **24**, 987–993.
BUSSEREAU, I., BELKHIRIA, M. S., GRAVEREAU, P., BOIREAU, A., SOUBEYROUX, J. L., OLAZCUAGA, R. & LE FLEM, G. (1992). *Acta Cryst.* C**48**, 1741–1744.
EL JAZOULI, A., SERGHINI, A., BROCHU, R., DANCE, J. M. & LE FLEM, G. (1985). *C. R. Acad. Sci.* **300**, 493–496.
FAIR, C. K. (1990). *MolEN. An Interactive Intelligent System for Crystal Structure Analysis.* Enraf–Nonius, Delft, The Netherlands.
FARGIN, E., BUSSEREAU, I., OLAZCUAGA, R., LE FLEM, G., CARTIER, C. & DEXPERT, H. (1994). *J. Solid State Chem.* **112**, 176–181.
GALESIC, N., MATKOVIC, B., TOPIC, M., COFFOU, E. & SLJUKIC, M. (1984). *Croat. Chem. Acta*, **57**(4), 597–608.
ISHIGURO, L., KITAZAWA, A., MITUZANI, N. & KATO, M. (1981). *J. Solid State Chem.* **40**, 170–174.
KEESTER, K. L. & JACOBS, J. T. (1974). *Ferroelectrics*, **8**, 657–664.
LAÜGT, M. (1973). *J. Appl. Cryst.* **6**, 299–301.
LE POLLES, G., EL JAZOULI, A., OLAZCUAGA, R., DANCE, J. M., LE FLEM, G. & HAGENMULLER, P. (1987). *Mater. Res. Bull.* **22**, 1171–1177.
LE POLLES, G., PARENT, C., OLAZCUAGA, R., LE FLEM, G. & HAGENMULLER, P. (1988). *C. R. Acad. Sci.* **306**, 765–768.
LOUËR, D. & LANGFORD, J. I. (1988). *J. Appl. Cryst.* **21**, 430–437.
MATKOVIC, B., PRODIC, B. & SLJUKIC, M. (1968). *Bull. Soc. Chim. Fr.* 1777–1779.
MATKOVIC, B., PRODIC, B., SLJUKIC, M. & PETERSON, S.W. (1968). *Croat. Chem. Acta*, **40**, 147–160.
MATKOVIC, B., PRODIC, B., SLJUKIC, M., TOPIC, M., WILLET, R. D. & PULLEN, F. (1970). *Inorg. Chim. Acta*, **4**, 571–576.
MARINDER, B. O. & WAHLSTRÖM, E. (1984). *Chem. Scr.* **23**, 157–160.
MBANDZA, A., BORDES, E. & COURTINE, P. (1987). *Mat. Res. Bull.* **20**, 251–257.
MCCARRON, E. M., CALABRESE, J. C. & SUBRAMANIAN, M. B. (1987). *Mater. Res. Bull.* **22**, 1421–1426.
RODRIGUEZ-CARVAJAL, J. (1990). Collected Abstracts of Powder Diffraction Meeting, Toulouse, France, July 1990, p. 127.
SCHMID, W. F. & MOONEY, R. W. (1964). *J. Electrochem. Soc.* **111**, 668–673.
SERGHINI, A. (1984). Thesis, University of Rabat (Morocco).
SERGHINI, A., BROCHU, R., GRAVEREAU, P. & OLAZCUAGA. R. (1995). To be published.
SERGHINI, A., KACIMI, M., ZIYAD, M. & BROCHU, R. (1988). *J. Chim. Phys. Chim. Biol.* **85**(4), 449–504.
SWANSON, H. E. & FUYAT, R. K. (1953). *Natl. Bur. Stand. (US) Circ.* **539**, 23–25.
YAO, P. C. & FRAY, D. J. (1983). *Solid State Ion.* **8**, 35–42.

Acta Cryst. (1995). B**51**, 913–920

Electron Density – Structure Relationships in Some Perovskite-Type Compounds

BY J. R. HESTER* AND E. N. MASLEN

Crystallography Centre, University of Western Australia, Nedlands 6907, *Australia*

(*Received* 20 *June* 1994; *accepted* 8 *March* 1995)

Abstract

Experimentally measured electron-deformation densities for the structurally related compounds dipotassium palladium tetrachloride, K_2PdCl_4, dipotassium silicon hexafluoride, K_2SiF_6, dipotassium palladium hexachloride, K_2PdCl_6, and dipotassium nickel tetrafluoride, K_2NiF_4, contain significant features in interatomic regions. The topographical relationship of interatom depletions to the structural geometry indicates that they originate from non-bonded interactions between atoms. The $\Delta\rho$ maps for K_2PdCl_4 and K_2PdCl_6 show unexpected structure near the K atoms. Low-temperature studies on K_2SiF_6 and K_2PdCl_4 indicate that these features are not due to anharmonic thermal motion, in marked contrast to those near the halide atoms. For the new low-temperature analysis included in the study: K_2SiF_6, cubic, $Fm\bar{3}m$, $M_r = 220.27$, $a = 8.046\,(2)$ Å, $V = 520.9\,(4)$ Å^3, $Z = 4$, $D_x = 2.81\,(2)$ Mg m^{-3}, μ(Mo $K\alpha$) = 2.09 mm^{-1}, $F(000) = 424$, $T = 110$ K, $R = 0.070$, $wR = 0.024$, $S = 1.47\,(9)$ for 129 independent reflections.

Introduction

Most accurate diffraction imaging studies focus on bonding-related deformation of the electron density near the shorter interatom vectors linking atomic nuclei. Several previous studies of simple inorganic compounds have reported significant accumulation and depletion in regions further from the nuclei. Electron-difference-density features persist in these regions even when the structure refinement model includes local multipole expansions of the electron density.

Maslen & Spadaccini (1989) identified consistent trends at structural cavities in measured $\Delta\rho$ maps for a series of transition-metal perovskite compounds. Their findings were confirmed and amplified in studies of $KCuF_3$ by Buttner, Maslen & Spadaccini (1990), and of $KZnF_3$ by Maslen, Spadaccini, Ito, Marumo, Tanaka & Satow (1993), who also identified $\Delta\rho$ depletions around the structural cavities.

Such evidence is frequently ignored or attributed to random experimental error and/or accumulation of systematic error near special positions. The possibility that these features are related to random errors can be investigated by replicating experiments. Accumulation of error at special positions cannot explain extended interatomic

* Present address: National Institute for Research in Inorganic Materials, Namiki 1-1, Tsukuba, Ibaraki 305, Japan.